



**IRON EVALUATION TESTS FOR MAIN RING MAGNET**  
**R. Yamada**  
**May 6, 1969**

We have been evaluating iron for the main ring magnet since the fall of 1967<sup>1)</sup>. In the spring of 1968 we made a proposal to most of the big steel companies in the USA to make sample iron laminations, which were to be decarburized and blue steamed, for the main ring magnet according to the specifications<sup>2)</sup>. Five companies: Armco Steel Company, Bethlehem Steel Company, Inland Steel Company, Republic Steel Company and U.S. Steel Company responded to our proposal. They delivered to us about 5 tons of laminations each.

Since then we have tested these laminations in several different ways. We tested laminations using an Epstein square measurement device and measured the interlamination resistance of blue steam coating. We punched B2 laminations for a magnet core about 1 foot long from each group, assembled hybrid magnets, and compared the different groups by measuring the magnetic field from the injection to the saturation field.

Epstein Square Measurement

We took out 5 sheets of iron from different places in each 5 ton stack of iron. From each sheet twenty sample strips (about 3 cm x 30 cm) were cut parallel to the rolling direction and another twenty were cut perpendicular to it. These samples were tested with an Epstein square device<sup>3)</sup>. The results are shown in Table 1. Five samples from each group were tested individually and the average values for

each group are shown in the table. The correction due to absolute calibration of flux density has not yet been applied to these data.

Iron A has the lowest coercive force of order 0.85 oersted and Iron C has the highest of 2.45 oersteds. The other irons are clustered in the range of 1.5 to 1.8 oersteds.

The coercive forces of perpendicularly cut samples are bigger than those of ones cut parallel by 2 to 13% as shown in the table. This is due to the deformed domain shape and the larger number of walls in the perpendicularly cut samples.

The other test samples from Iron N, which were taken before and after the repassing process -cold rolling after annealing-, show clearly an increase of 22% in  $H_C$ . The repassed samples were stretched in the rolling direction and not annealed afterwards. These samples were a mixture of parallel and perpendicular cut due to the small number of samples.

The flux density of different irons at 100 oersteds ranges from 18.8 to 19.9 kG; at 200 oersteds from 20.1 to 21.2 kG; and at 400 oersteds from 21.6 to 22.7 kG. These values of flux density are expected to be brought down by 5% by a calibration in near future. At 400 oersteds Iron A has the highest flux density, Iron B and Iron G have the next highest, and the rest are almost in the same range, except for Iron H.

Almost all iron samples of parallel cut have higher magnetic induction than those of perpendicular cut. Especially

Iron A, which has the highest directional orientation, had differences of 0.8, 0.6, and 0.3 kG at 19.1, 20.6, and 22.4 kG respectively.

One sample from each group was baked in an oven at 150°C for a week to see the aging effect, the result is shown in Table 2. They showed an increase of coercive force about 5 ~ 20%, except Iron G. The percentage increase is biggest with Iron A and the Iron D shows the smallest increase.

#### Interlaminar Resistance Test

The surface of the laminations of most samples was steam blued at individual iron factories. The cost of blue steaming is much cheaper than the cost of coating, and we could save time and money by doing blue steaming.

The repetition cycle of the 200 BeV machine is one every few seconds, so we do not need an interlamination resistance as high as a fast cycling machine does. The interlamination resistance was measured in the following way: two different samples of punched laminations about a foot long were stacked together on a stacking jig and pressure was applied. The laminations were insulated electrically from the stacking jig and a current of 20 A was passed through the lamination from one end of the stack to the other end. The voltage drop over two inches along the length was measured at several different pressures. The pressure in the production magnet is expected to be about 100 psi.

The measured minimum resistance  $\rho$  ( $m\Omega cm^2$ ) are shown in Table 3. The maximum values in  $\rho$  were usually up to twice as much as the minimum values. After several pressure cycles, the resistance was measured and the change of the resistance during a cycle is shown in the table. If we take as an acceptable minimum  $30 m\Omega cm^2$  at 220 psi, Iron F is not satisfactory but other seem acceptable.

The difference in length of the stack due to the change in pressure from 118 to 253 psi was less than 0.1%; the stacking factor may change that much.

The bare laminations and the laminations coated with manganese phosphate of the Iron G was measured in the same way. The resistance of the bare one was  $4.5 m\Omega cm^2$ , and that of the coated one was  $2.5 \Omega cm^2$  at about 100 psi.

#### Magnetic Field Measurement

Three foot hybrid magnets were assembled using three different iron laminations of one foot each, in the same way as was shown in a previous report<sup>4)</sup>. The excitation curve, the magnitude of the remanent field, the gradient distribution at injection field and saturation field were measured.

The excitation curves of the magnet iron were measured using a current shunt and a calibrated search coil and integrator system. The output voltages of these two parameters were put into two DVM's, and readings were read simultaneously. Due to the noise coming from SCR's in the power supply, we could not get good signals from the current shunt when pulsing the

magnet, Therefore we could not get an excitation curve of pulsed mode through the data acquisition system. But later we excited the magnet gradually in semi-pulsed mode, filtering the noise through a filter in the DVM, and measured the excitation curve, through the data acquisition system. Amp factor - deviation of excitation curve from the initial linear slope - was also calculated through the computer on-line. The amp factors at different excitation levels are shown in Table 4, with their respective stacking factors. The stacking factor is about 99.0%. Typical excitation curve of Iron A is shown in Fig. 1.

The magnitude of remanent field after excitation of 22.5 kG is shown in Table 5, and compared to its respective coercive force. Also the ratio of remanent field to coercive force is given. It is about 9 to 10, which corresponds to the ratio of the magnetic path in iron and gap height. The remanent field, of 9 kG excitation is about 10% less than that of 22.5 kG.

The gradient distributions were measured with a twin search coil and integrator system in a DC magnetic field as reported in a previous report<sup>4)</sup>. But the system was computerized, so that the motion of the probe is controlled by a Varian 620/i computer, and the output of search coil was put into the computer through the system of a sample and hold circuit and an AD converter. The gradient distribution

$$k(x) = \frac{1}{B(o)} \frac{dB}{dx}, \quad (m^{-1})$$

was calculated on-line and the curves were plotted through a Calcomp plotter.

The results of the measurements on the median plane are shown in Fig. 2 through Fig. 9. We used the same B2 magnet coil as in the previous report<sup>4)</sup>. The strong field variation near the coil is due to the gaps between the copper conductors and iron. The most important information between these curves is the change in the magnitude of sextupole terms at the center of different iron at different field levels are shown in Table 6.

The sextupole term at low field, including injection field, is determined by the coercive force. They are quite linearly correlated, as can be seen in the table. It is highly preferable to use iron for the magnet which has a coercive force less than 1 oersted. The variation in the coercive force should be kept to a minimum. It should be less than  $\pm 0.1$  oersted. If it is bigger than that, the adjustments of the correction magnets seems too complicated. Iron A and Iron G seem preferable irons from this point.

In the high field region from 9 to 18 kG, corresponding to 200 and 400 BeV respectively, there is not much difference between any of the sample laminations, as can be seen from Table 6.

At saturation field Iron F shows better gradient distributions than the rest of the samples. The averaged  $\mu$  is also shown in the table for comparison. The correlation between

the sextupole term and  $\mu$  value is not clear from these data.

Miscellaneous

Rockwell hardness test B was done on one lamination of each iron, and the average number of several points is shown in Table 7.

---

Table 7      Rockwell Hardness Test B							
Iron A	Iron B	Iron C	Iron D	Iron E	Iron F	Iron G	Iron H
24	37	41	44	54	56	26	47

---

Iron A and Iron G are much softer than others as shown in the table and the punched surface of Iron A is the worst of all. The surface has bigger breaks and more burrs, and the top edge of the punched surface is waviest. Even its regular surface is the roughest of all. These facts may be due to the softness and bigger grain size.

The crown of sample lamination was measured and the averaged values of 5 laminations each are shown in Fig. 10. Iron D and Iron E have a crown bigger than 1%, but the rest have a crown less than 1%. We had to use more shims at the sides for the laminations of Iron D and E due to the bigger crown.

Conclusions

The magnet should have a small sextupole term at the injection field of 500 gauss. If the coercive force of the iron is one oersted or less, the sextupole term can easily

be corrected by the correction coils. Also the variation in the coercive force should be kept to a minimum.

In the intermediate field from 9 to 18 kG, there is not much difference between any iron laminations in the shape of gradient distribution. In the saturation region up to 22.5 kG, there is some difference between the laminations. The sextupole term in this region should be reduced or cancelled by incorporating crenellation in the laminations or by the use of high field correction coils.

From these considerations, Iron A and Iron G seem good candidates for the main ring magnet. Iron A has a smaller coercive force of 0.85 oersted, compared to 1.00 oersted of Iron G. Both irons are quite soft, but the Iron A shows worse punchability than Iron G. The magnitude of crown of both irons seem about the same.



References

- 1) J.W. DeWire, Miscellaneous Notes on Steel and Laminations for the Main Ring Magnets, National Accelerator Laboratory report EN-99 0420, Feb. 5, 1968.
- 2) F.C. Shoemaker, Main Ring Magnet Iron, National Accelerator Laboratory report ES-2 0420, May 30, 1968.
- 3) Will be reported later.
- 4) R. Yamada, DC Field Measurements of No. 2 Model Magnet, National Accelerator Laboratory report TM-82 0423, Sept, 27, 1968.

Table 1 Epstein Square Measurement

	Cut	Density	H ~ 100 oe		H ~ 200 oe		H ~ 400 oe		Difference in Hc
			Hc (oe)	B (kG)	Hc (oe)	B (kG)	Hc (oe)	B (kG)	
Iron A	//	7.873	0.82±.05	19.9±.2	0.83±.02	21.2±.1	0.82±.05	22.7±.2	7%
"	⊥	7.866	0.89±.04	19.1±.1	0.88±.02	20.6±.1	0.88±.02	22.4±.1	
Iron B	//	7.859	1.60±.16	19.8±.2	1.60±.16	21.0±.1	1.60±.17	22.5±.2	2%
"	⊥	7.865	1.63±.13	19.5±.3	1.63±.15	20.8±.2	1.62±.14	22.4±.2	
Iron C	//	7.870	2.41±.03	19.7±.1	2.42±.04	20.9±.1	2.41±.02	22.4±.2	2%
"	⊥	7.879	2.48±.03	19.5±.2	2.47±.03	20.9±.2	2.46±.06	22.4±.2	
Iron D	//	7.860	1.47±.24	19.5±.3	1.47±.24	20.8±.3	1.47±.19	22.3±.4	6%
"	⊥	7.865	1.55±.19	19.1±.2	1.55±.19	20.5±.1	1.56±.18	22.2±.1	
Iron E	//	7.849	1.67±.05	19.5±.1	1.67±.05	20.8±.1	1.67±.06	22.4±.3	8%
"	⊥	7.823	1.80±.01	19.1±.2	1.80±.03	20.4±.2	1.80±.02	22.2±.2	
Iron F	//	7.834	1.44±.04	19.2±.2	1.44±.05	20.7±.1	1.45±.05	22.3±.1	5%
"	⊥	7.852	1.52±.05	19.1±.2	1.51±.05	20.4±.2	1.51±.05	22.2±.1	
Iron G	//		0.94	19.5	0.94	20.9	0.94	22.5	13%
"	⊥		1.07	19.5	1.06	20.9	1.06	22.4	
Iron H	//		2.30	19.3	2.31	20.6	2.31	22.0	0%
"	⊥		2.33	18.8	2.30	20.1	2.31	21.6	
Iron N mixed (non repassed)		7.877	1.55	19.4	1.55	20.8	1.55	22.5	22%
Iron N mixed (repassed)		7.877	1.85	19.2	1.92	20.5	1.90	22.3	

Difference in Hc

Table 2 Aging Effect on Epstein Square Samples

Sample	Cut	H ~ 100 oe				H ~ 200 oe				H ~ 400 oe			
		Hc (oe)		B (kG)		Hc (oe)		B (kG)		Hc (oe)		B (kG)	
		Before	After	Before	After	Before	After	Before	After	Before	After	Before	After
Iron A	//	0.81		19.9		0.83		21.3		0.83		22.8	
			0.91		19.9		0.92		21.4		0.94		22.9
"	L	0.87		19.0		0.87		20.5		0.87		22.3	
			1.02		19.0		1.05		20.5		1.03		22.2
Iron B	//	1.58		19.8		1.59		21.0		1.59		22.6	
			1.64		20.8		1.65		21.1		1.65		22.7
"	L	1.63		19.6		1.64		20.9		1.65		22.5	
			1.74		19.6		1.75		21.0		1.77		22.6
Iron C	//	2.40		19.7		2.43		20.9		2.41		22.4	
			2.58		19.8		2.54		21.0		2.60		22.4
"	L	2.46		19.6		2.44		20.9		2.46		22.5	
			2.53		19.7		2.55		21.0		2.58		22.6
Iron D	//	1.41		19.5		1.40		20.9		1.40		22.4	
			1.40		19.6		1.41		21.1		1.43		22.5
"	L	1.47		19.1		1.47		20.5		1.47		22.1	
			1.47		19.2		1.53		20.6		1.53		22.1
Iron E	//	1.67		19.6		1.66		20.8		1.66		22.4	
			1.79		19.4		1.80		20.6		1.78		22.1
"	L	1.79		19.1		1.79		20.4		1.78		22.2	
			1.90		19.1		1.92		20.5		1.89		22.3
Iron F	//	1.43		19.4		1.42		20.7		1.42		22.3	
			1.55		19.2		1.54		20.4		1.55		22.2
"	L	1.51		19.9		1.50		20.4		1.50		22.3	
			1.64		19.2		1.65		20.5		1.66		22.2
Iron G	L	1.05		19.3		1.06		20.8		1.05		22.5	
			1.04		19.4		1.04		20.7		1.04		22.4

Table 3 Minimum Interlaminar Resistance  $\rho$  ( $m\Omega cm^2$ )

pressure (psi)	Iron A	Iron B	Iron C	Iron D	Iron E	Iron F
118	29.9	72.5	69.7	122.6	171.2	11.7
235	29.3	63.6	47.0	81.7	134.1	11.9
294	23.5	62.9	46.2	65.6	108.8	11.0
353	23.2	63.9	39.5	57.0	98.4	10.8
235	24.4	67.1	43.8	64.6	106.3	10.8
118	33.4	82.9	67.1	102.4	138.6	13.1
Colour of Surface	Charcoal	Straw	Black	Straw ~ Bluish	Black	Bluish

Table 4 Amp Factors and Stacking Factors

	Stacking Factor	Amp Factors		
	%	18kG	20kG	22.5kG
Iron A	99.2	1.037	1.087	1.207
Iron B	98.9	1.033	1.080	1.191
Iron C	99.0	1.037	1.081	1.198
Iron D	98.6	1.039	1.091	1.228
Iron E	98.6	1.038	1.084	1.206
Iron F	98.7	1.035	1.081	1.200
Iron G	99.0	1.032	1.072	1.191
Iron H				

Table 5 Magnitude of Remanent Field and Average Coercive Force

	Coercive Force in Oersted	Remanent Field in Guass	Ratio of R.F./C.F.
Iron A	0.85	8.4	9.9
Iron B	1.61	16.7	10.4
Iron C	2.44	23.9	9.8
Iron D	1.52	13.5	8.9
Iron E	1.74	55.6	9.0
Iron F	1.48	12.6	8.5
Iron G	1.00	11.5	11.5
Iron H	2.31	25.0	10.8

Table 6 Magnitude of Sextupole Term

	$H_c$ at 400 oe	0.5kG	1kG	9kG	18kG	21kG	22kG	22.5kG	$\mu$ at 400 oe
Iron A	0.85	-.57	-.37	-.08	-.19	+.33	+1.93	+2.87	56.7
Iron B	1.61	-1.61	-.63	-.06	-.19	+.38	+2.17	+3.07	56.4
Iron C	2.44	-2.22	-.83	-.08	-.26	+.19	+2.09	+2.91	56.3
Iron D	1.52	-1.56	-.65	-.08	-.16	+.39	+2.07	+3.09	55.9
Iron E	1.74	-1.97	-1.08	-.08	-.16	+.28	+2.13	+3.01	55.9
Iron F	1.48	-1.42	-.69	-.10	-.24	+.12	+1.61	+2.48	55.8
Iron G	1.09	-.76	-.31	-.20	-.24	+.15	+2.15	+3.19	57.0
Iron H	2.44	-1.85	-1.10	-.06	-.14	+1.04		+4.25	55.0

$\frac{1}{B_0} \frac{\partial^2 B}{\partial x^2}$  ( $m^{-2}$ )

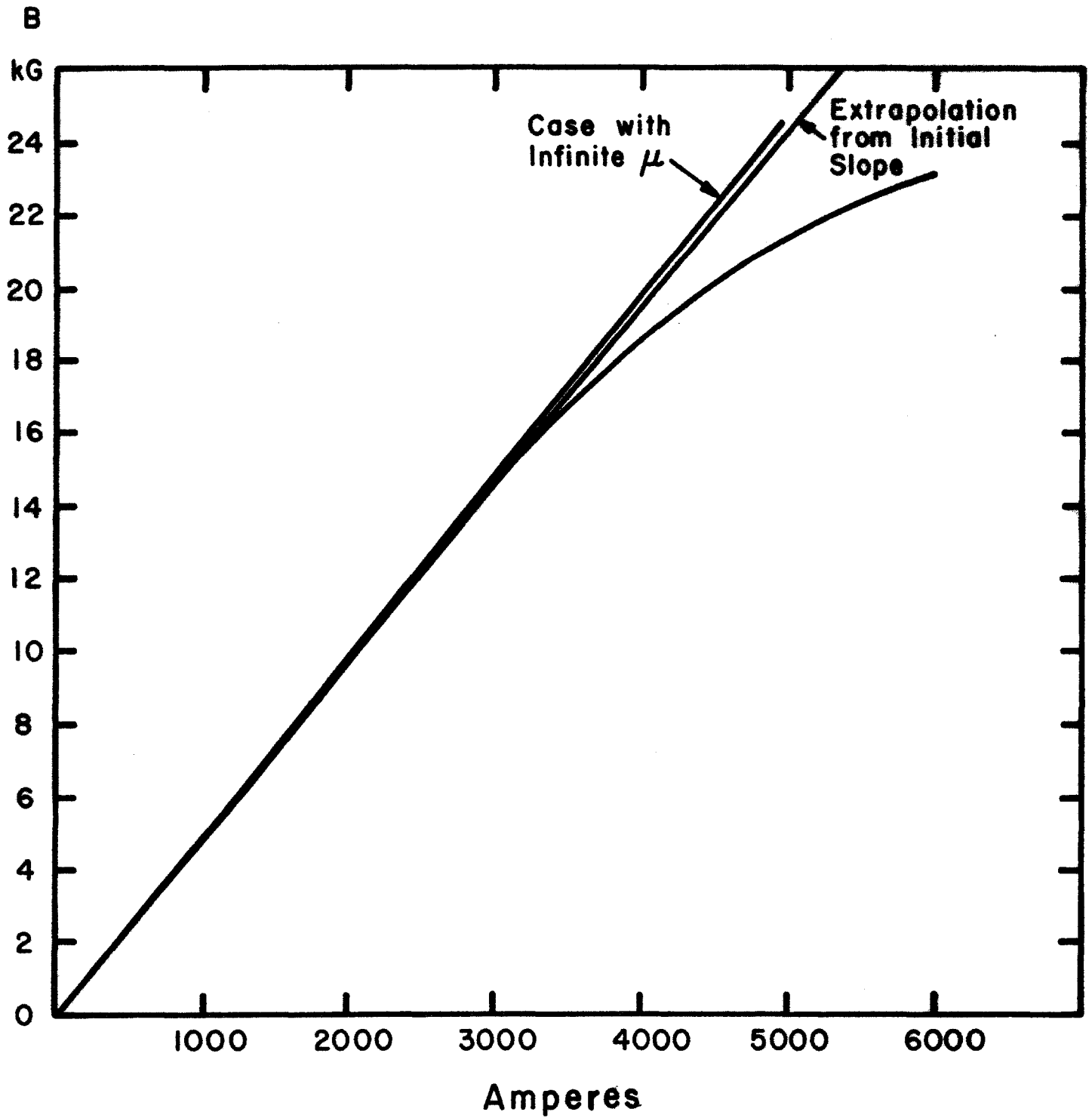


Fig.1 Excitation Curve of Iron A

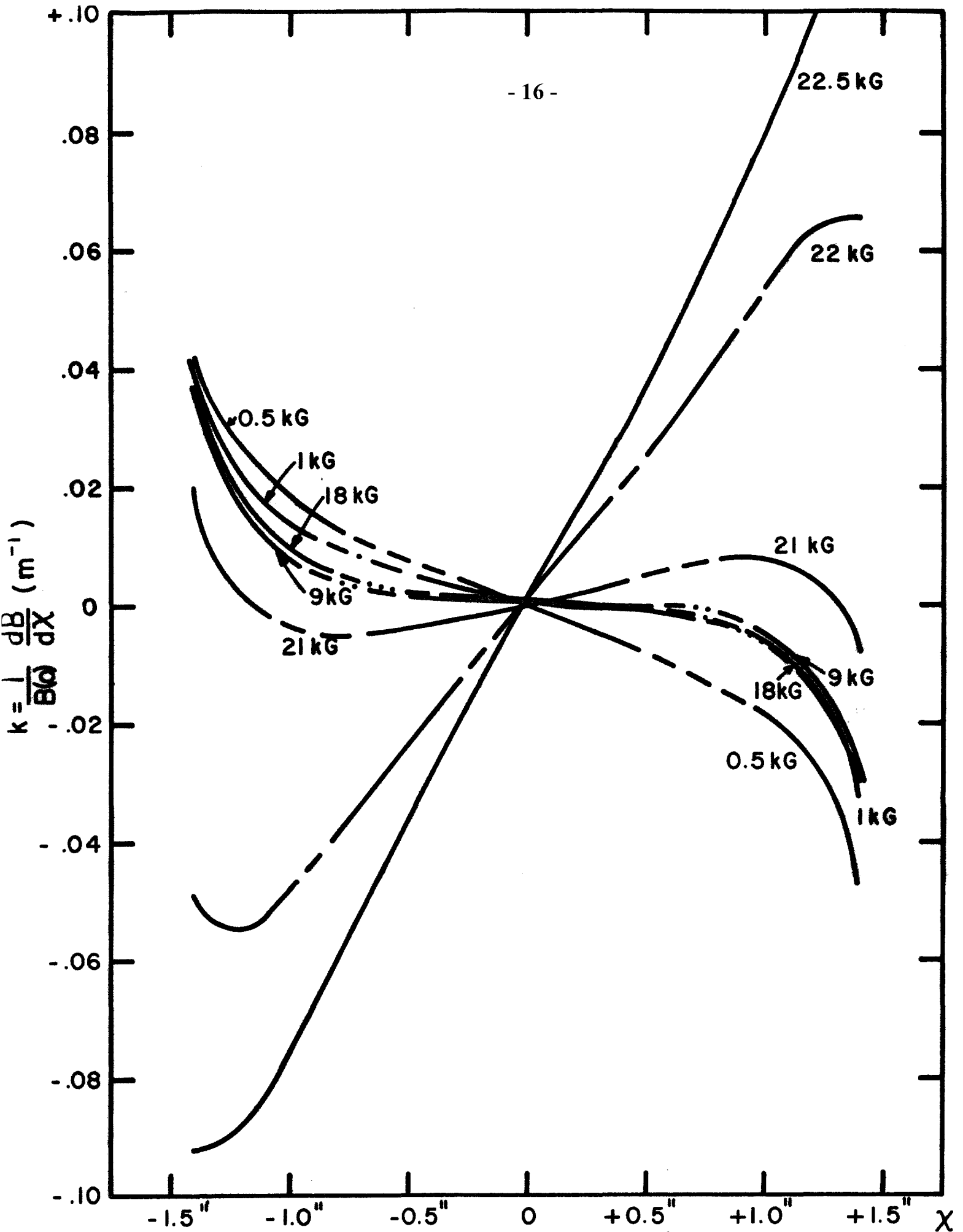


Fig. 2 Gradient Curve of Iron A



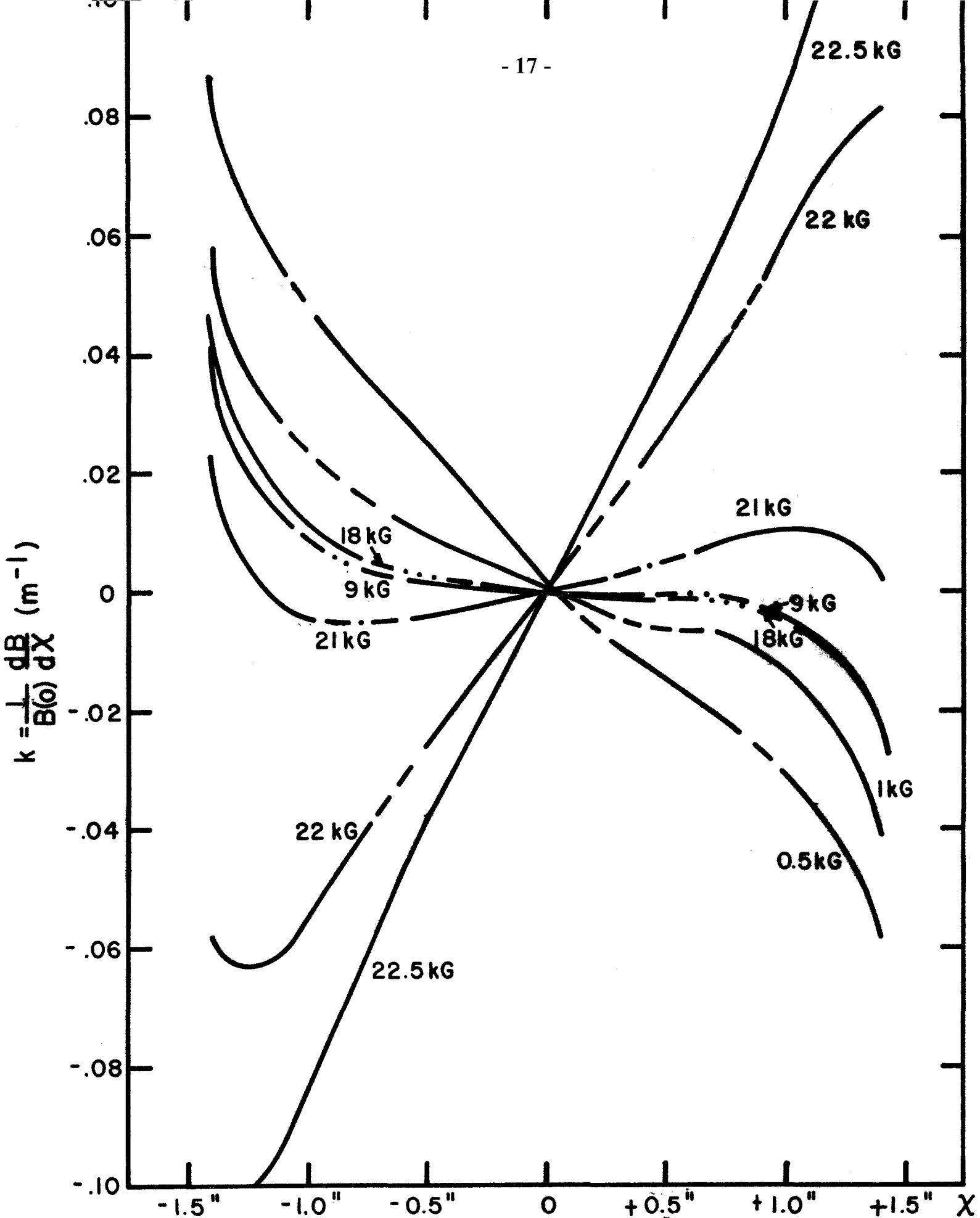


Fig. 3 Gradient Curve of Iron B

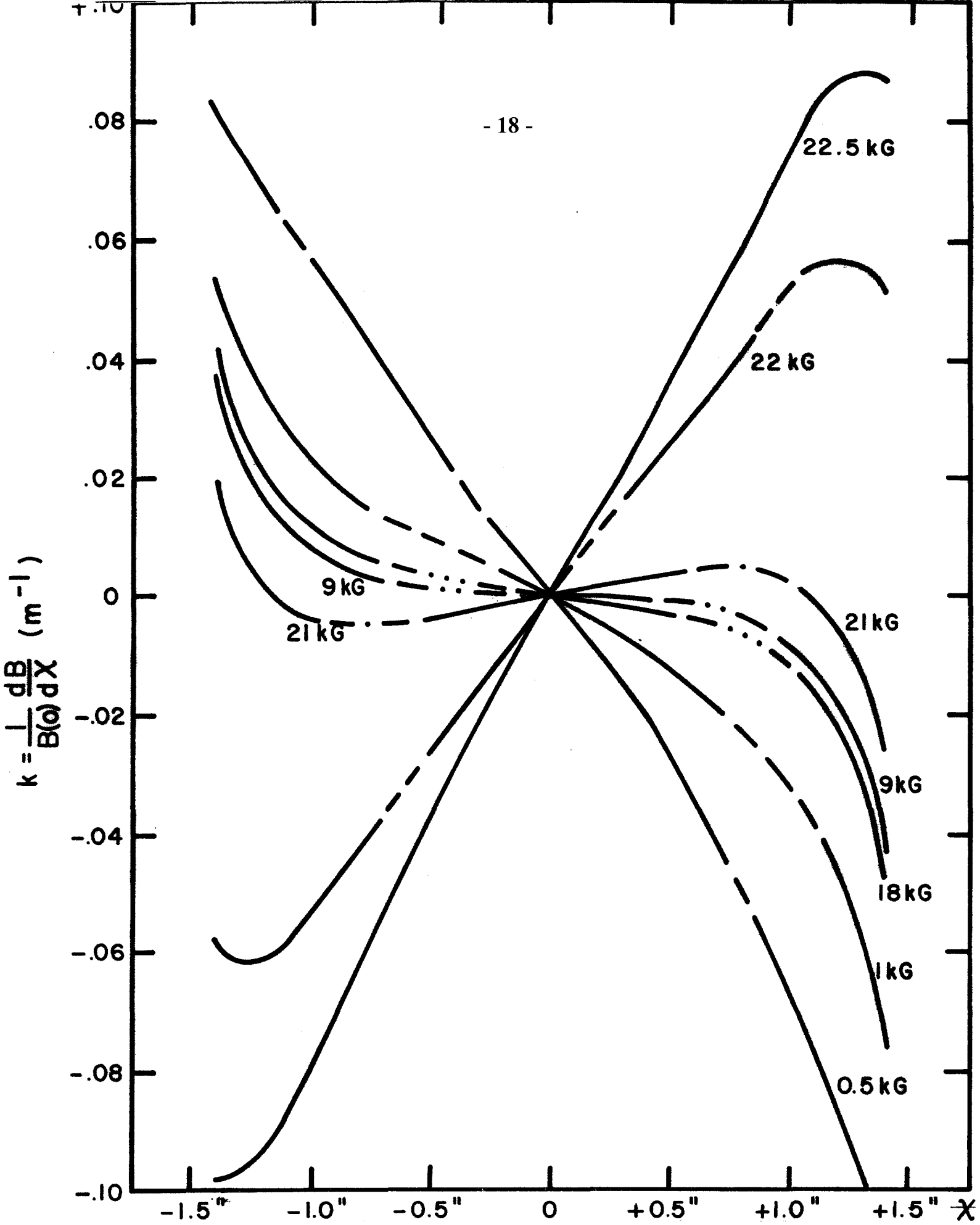


Fig. 4 Gradient Curve of Iron C

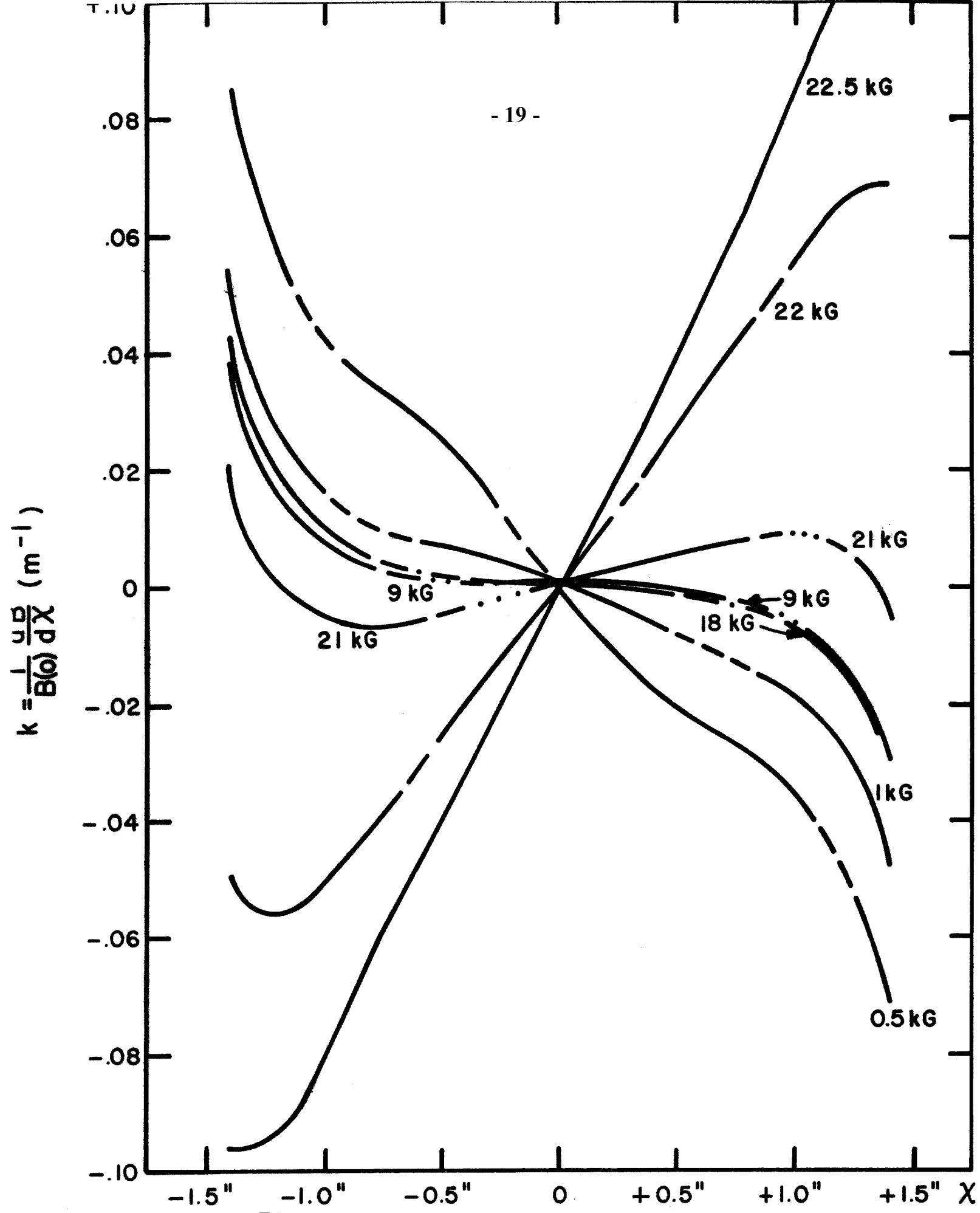


Fig. 5 Gradient Curve of Iron D

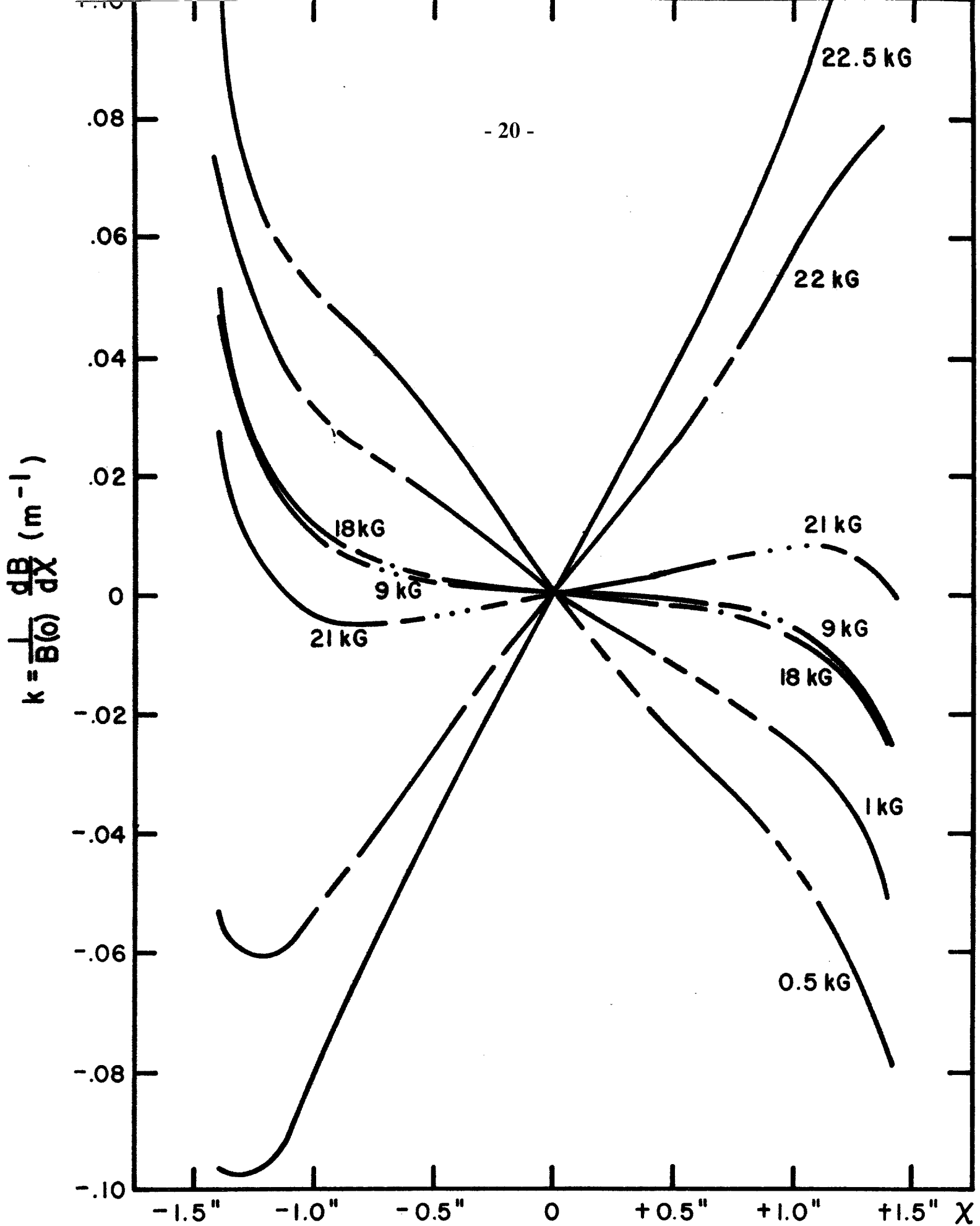


Fig. 6 Gradient Curve of Iron E

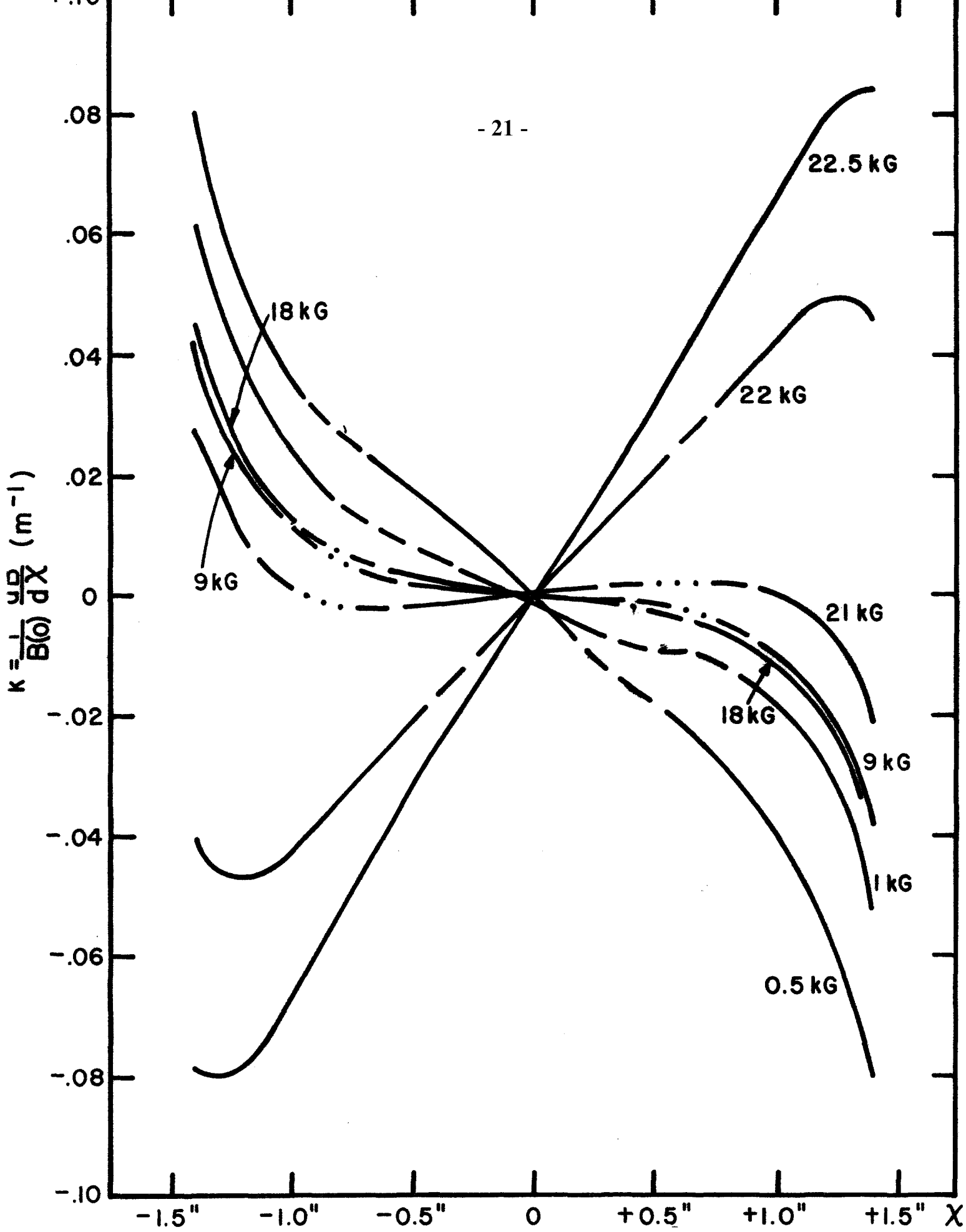


Fig. 7 Gradient Curve of Iron F

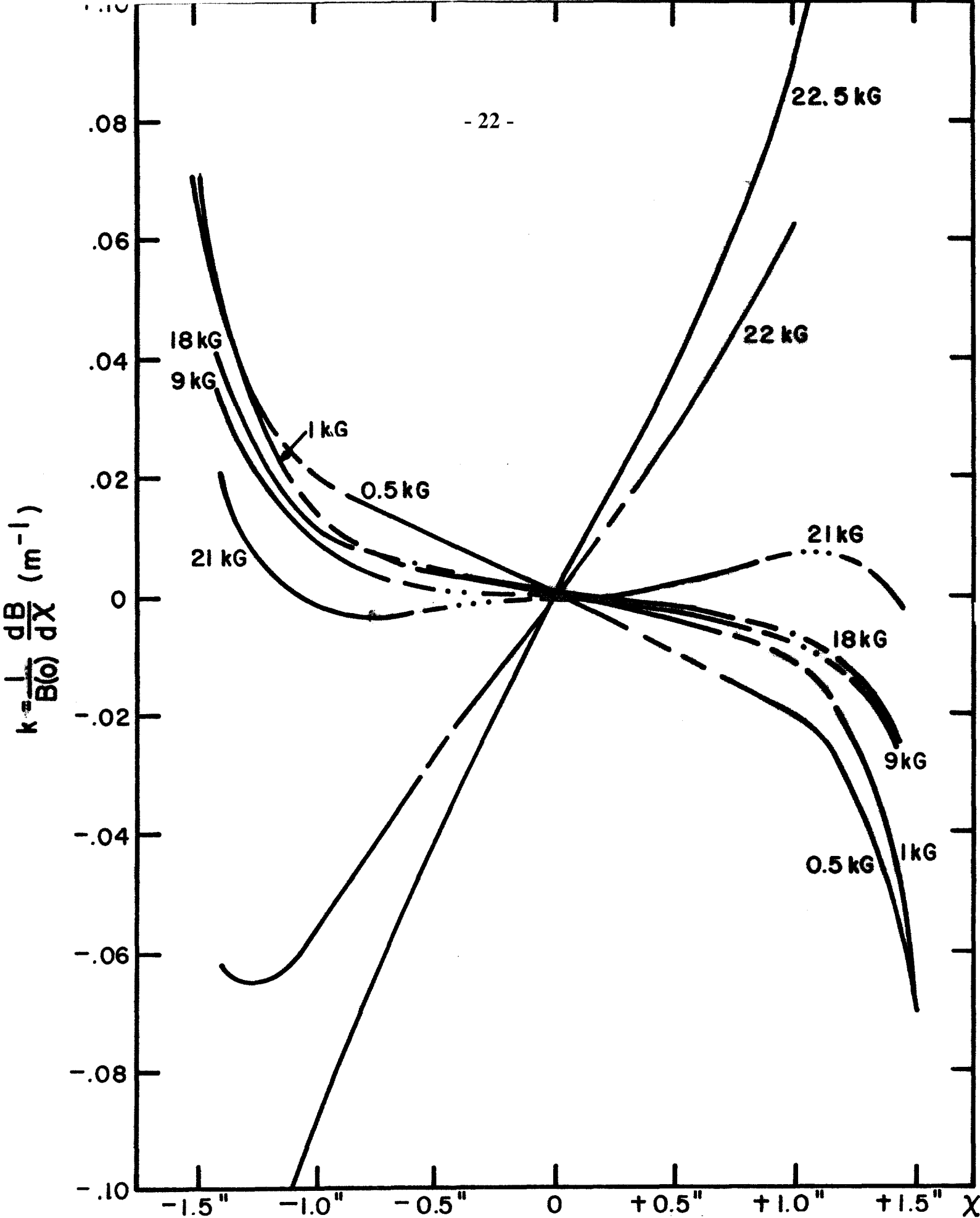


Fig. 8 Gradient Curve of Iron G

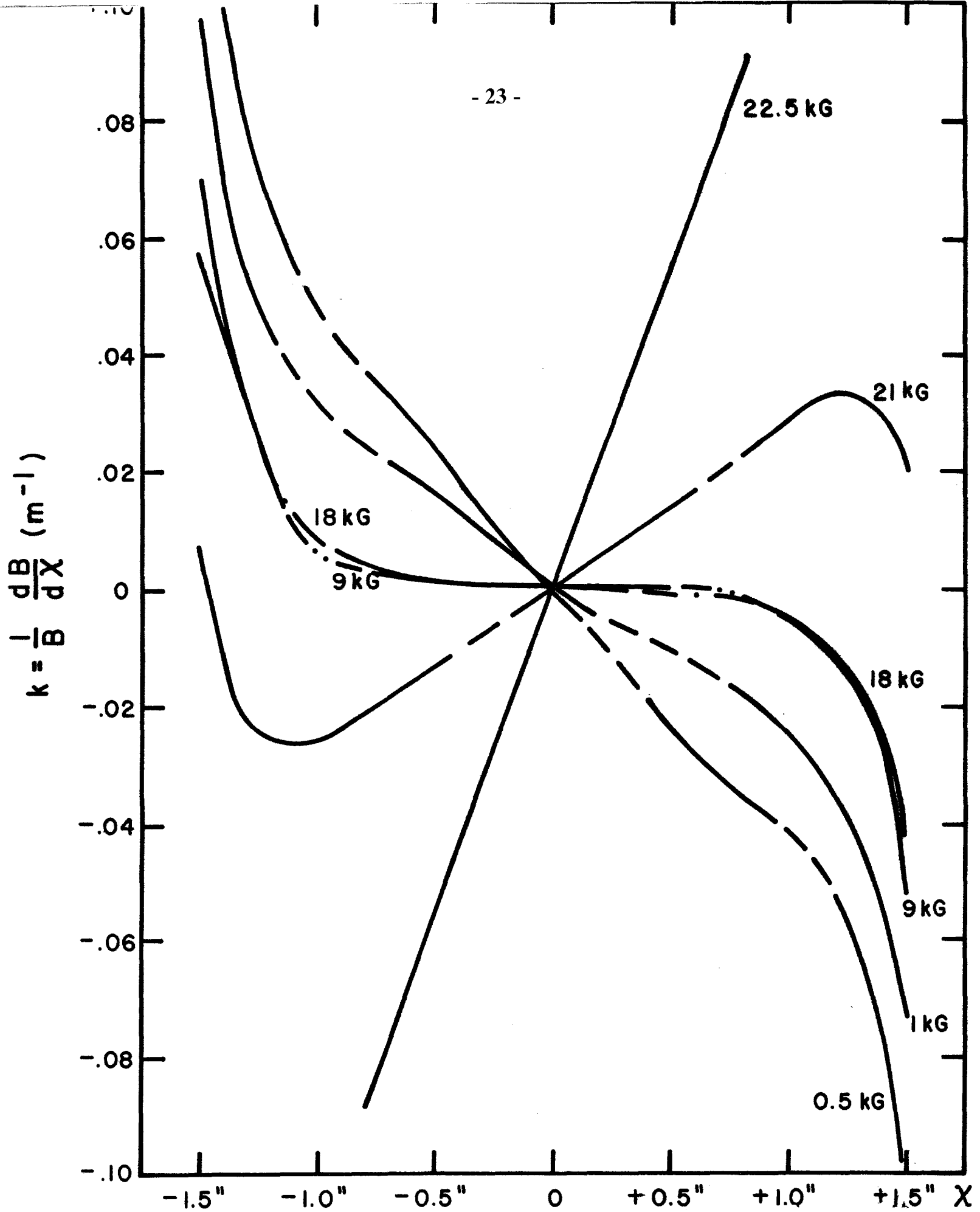


Fig. 9 Gradient Curve of Iron H

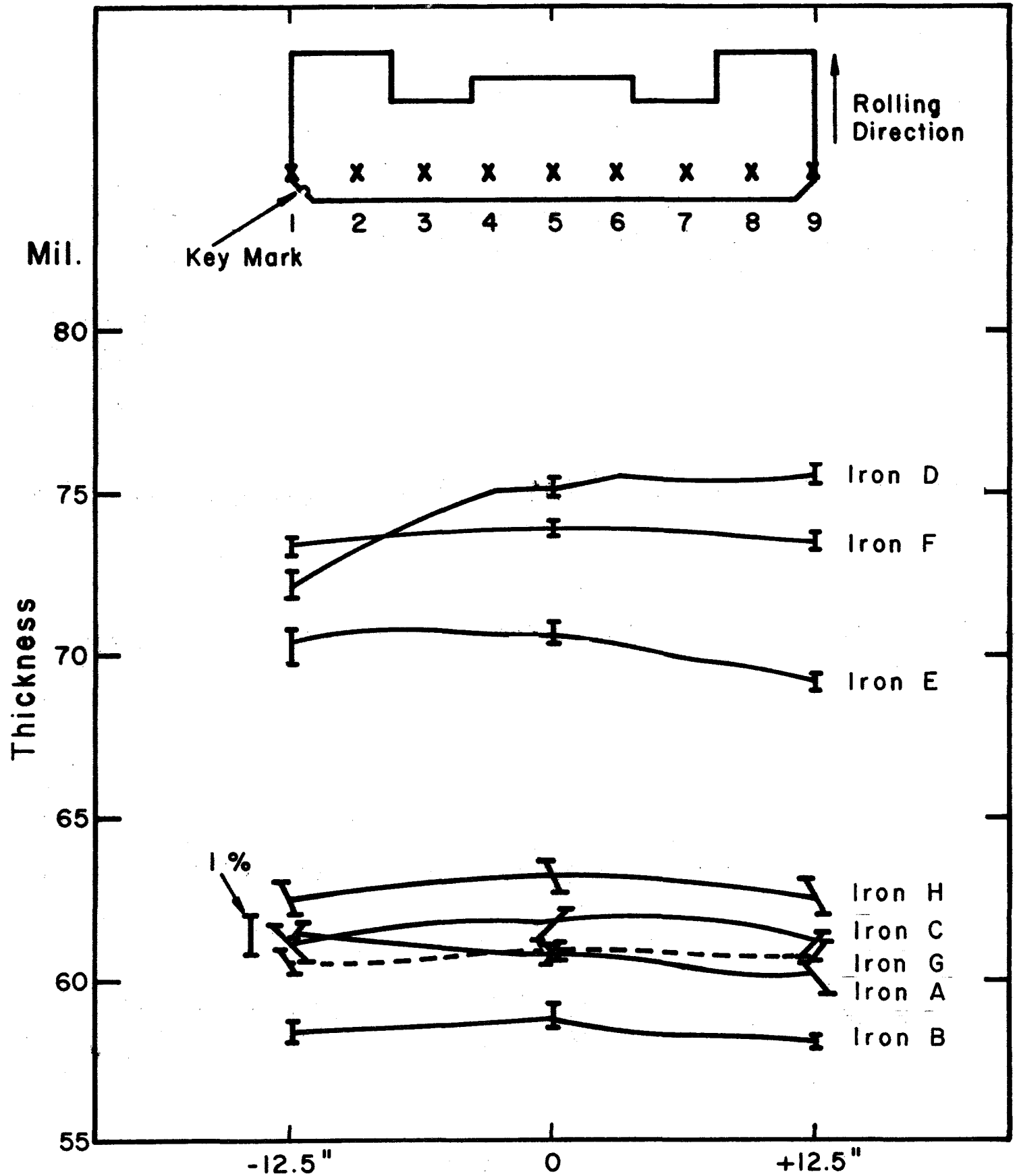


Fig. 10 Thickness Variation Across Lamination